Curcumin as a potential multiple-target inhibitor against SARS-CoV-2 infection: A detailed interaction study using quantum chemical calculations

SUMIT KUMAR*

Department of Chemistry, Magadh University, Bodh Gaya-824234, Bihar, India

Abstract: Curcumin is one of the important naturally occurring compounds having several medicinal properties such as: antiviral, antioxidant, antifibrotic, antineoplastic as well as anti-inflammatory. SARS-CoV-2 has emerged as infectious virus, which severely infected a large number of people all over the world. Many efforts have been made to prepare novel antiviral compound, but it is still challenging. Naturally occurring compound, curcumin, can be used as an alternative to antiviral compound against SARS-CoV-2. Its effect against SARS-CoV-2 is already highlighted in the literature. But the quantitative study of its interaction with various precursors of SARS-CoV-2 is not reported till date. This paper reports the interaction of curcumin with angiotensin-converting enzyme2, transmembrane serine protease 2, 3-chymotrypsin-like protease and papain-like protease through molecular docking and quantum chemistry calculations to achieve quantitative understanding of underlying interactions. Here the conformational flexibility of curcumin is also highlighted, which helps it to accommodate in the four different docking sites. The study has been performed using calculations of geometrical parameter, atomic charge, electron density, Laplacian of electron density, dipole moment and the energy gap between highest occupied and lowest unoccupied molecular orbitals. The non-covalent interaction (NCI) analysis is performed to visualize the weak interaction present in the active sites. Combinedly molecular docking and detailed quantum chemistry calculations revealed that curcumin can be adopted as a potential multiple-target inhibitor against SARS-CoV-2.

Keywords: antiviral drug; non-covalent interaction; charge density analysis; atom-in-molecule calculation; angiotensin-converting enzyme2; transmembrane serine protease 2.

---

* E-mail: sumitkrmgr@gmail.com

381

INTRODUCTION

In the last couple of years, coronavirus 2 (SARS-CoV-2) widely spread and affected over more than 600 million population of the world and 6.5 million people died according to world health organization (https://www.who.int/). Considering this situation world health organization already characterized it as pandemic in 2020. In comparison to middle east respiratory syndrome coronavirus (MERS-CoV), SARS-CoV-2 has been found more contagious and therefore spread fast through population.[1] The development of novel antivirals against SARS-CoV-2 is a matter of great interest as well as a challenge ahead of the scientific community. A great effort has been made to validate antiviral compounds. Some naturally occurring compounds already have antiviral properties, thus can be used as an alternative to antiviral complex compounds evolved during the development of novel antivirals.[2,3] Curcumin, a yellow pigmented polyphenolic compound, majorly found in turmeric and used as a food additive.[4] Its antiviral activity against SARS-CoV-2 along with other viral infections are already reported in the literature.[5–9] It is an interesting naturally occurring substance, which has antioxidant, antifibrotic, antineoplastic as well as anti-inflammatory properties.[4,10]

SARS-CoV-2 belongs to fusion protein containing two major subunits (S1 and S2).[11] For the spread of SARS-CoV-2, angiotensin-converting enzyme2 plays a major role determining its entry through interaction with viral spike protein.[11,12] Further transmembrane serine protease 2 (TMPRSS2) cleaves the spike protein into smaller subunits, which leads to subsequent cellular entry of infectious viral RNA.[13–16] Upon entry to the cell, two SARS-CoV-2 proteases 3--chymotrypsin-like protease (3CLpro, also known as main protease, Mpro) and papain-like protease (PLpro) cleaves the proteins.[13–16] Both 3CLpro and PLpro are essential for the release of 16 non-structural proteins (nsps) on breaking down polyprotein.[13–16] Further the replication and transcription occur to produce viral genomes by accumulation of infectious replicase on the host membrane.[17] Later the four major proteins: the spike (S) protein, membrane (M) protein, nucleocapsid (N) protein, and the envelope (E) protein form and leads to the formation of viral particle. Some viral particle of CoVs is also reported, without using full ensemble of all four proteins, by encoding extra protein having similar or compensatory ability.[18–20] Till date there is no report available in the literature providing in-depth molecular level study, of interaction of curcumin along with TMPRSS2, ACE2, PLpro and 3CLpro, to understand its ability to encounter with SARS-CoV-2. Therefore, the study of curcumin along with precursors of SARS--CoV-2 has been reported here to provide necessary information, which may be helpful to understand the applicability of curcumin in the treatment against SARS-CoV-2.

In the present study, not only the interaction of the curcumin with precursors of SARS-CoV-2 but also its conformational flexibility has been monitored to get the in-depth understanding related to the protein-ligand interaction. The study has been performed to monitor the distribution of electron density, dipole moment, atomic charge and atom-in-molecule (AIM) properties of curcumin in the gas phase as well as in the active sites of four different precursors related to SARS-CoV-2. The non-covalent interaction (NCI) analysis is performed for the visualization of weak interactions in the active sites. The NCI plot allows to study the macromolecular system effectively.

COMPUTATIONAL DETAILS

Molecular docking is the most famous tool to monitor the interaction of ligand and receptor.[21] It provides the useful information about the binding site of the protein used by the ligand to accommodate through various non-covalent interactions. The docking studies has been performed using computational software. AutoDock4 together with AutoGrid4 python programming-based tool has been used to study the molecular docking of curcumin with TMPRSS2, ACE2, PLpro and 3CLpro.[22,23] The docking uses the grid driven method to prepare grids around the protein and the lookup table for the simulation by calculating the energy keeping an atom as a probe on each of the grid points. The lookup table helps the simulation to effectively measure the binding energy of the conformers with the target protein. Further Lamarckian genetic algorithm has been used to search the lowest binding energy conformer associated in the local minima position close to the protein. AutoDock4 uses the semiempirical method to obtain the binding energies for the suitable conformers at the docking site of the protein in bound as well as unbound states. The study therefore provides interesting information about the reliable docking pose prediction for ligand protein interactions. PyMOL, LigPlot+ and Protein-ligand interaction profiler (PLIP) tools are used to draw the informative pictures of docking studies.[24-26] PLIP tool is also used here to identify the non-covalent interaction of curcumin with TMPRSS2, ACE2, PLpro and 3CLpro.

The efficacy of curcumin against the SARS-CoV-2 virus has been realized by studying the interaction of curcumin with TMPRSS2, ACE2, 3CLpro and PLpro. This interaction has been monitored using the docking studies. For these docking studies, crystal structures of TMPRSS2 (PDB ID: 1Z8A), ACE2 (PDB ID: 3D0G), PLpro (PDB: 3E9S), and 3CLpro (PDB ID: 3AW0) are used. These PDBs are obtained from Protein Data Bank (https://www.rcsb.org/).[27]

To understand the conformational flexibility of the curcumin, its diketone form in the gas phase is compared with the same obtained from the active sites of TMPRSS2, ACE2, PLpro and 3CLpro. Single point calculations are performed for curcumin obtained from active sites of TMPRSS2, ACE2, PLpro and 3CLpro whereas optimization has been performed to obtain the most stable geometry of curcumin in the gas phase at B3LYP/de2-TZVP level of theory. B3LYP is Becke's three-parameter exchange functional with the Lee–Yang–Parr correlation functional, which provides good result with reasonable error.[28] The def2-TZVP proposed by Ahlrichs–Weigend is triple-zeta valence with polarization basis set.[29] It provides better result than 6–311G**.[30,31] Furthermore, def2 basis sets are designed to deliver consistent accuracy for nearly all atoms up to radon.[30,32] These calculations are performed using Turbo mole version 7.6 *ab initio* quantum-chemical calculation software package.[33,34] The comparison has also been made based on the geometrical parameter, atomic charge, electron density, Laplacian of electron density, dipole moment and the energy gap between highest occupied and

lowest unoccupied molecular orbitals. NCI and AIM analysis are performed using NCI Plot and Turbomole version 7.6 software, respectively.[33-35]

RESULTS AND DISCUSSION

The docking studies of curcumin have been performed with TMPRSS2, ACE2, PLpro and 3CLpro, which are related to coronavirus 2 (SARS-CoV-2). For these docking studies, ten rotatable bonds of curcumin are used. The lowest binding energy docking pose of curcumin with TMPRSS2, ACE2, PLpro and 3CLpro are shown in Fig. 1.
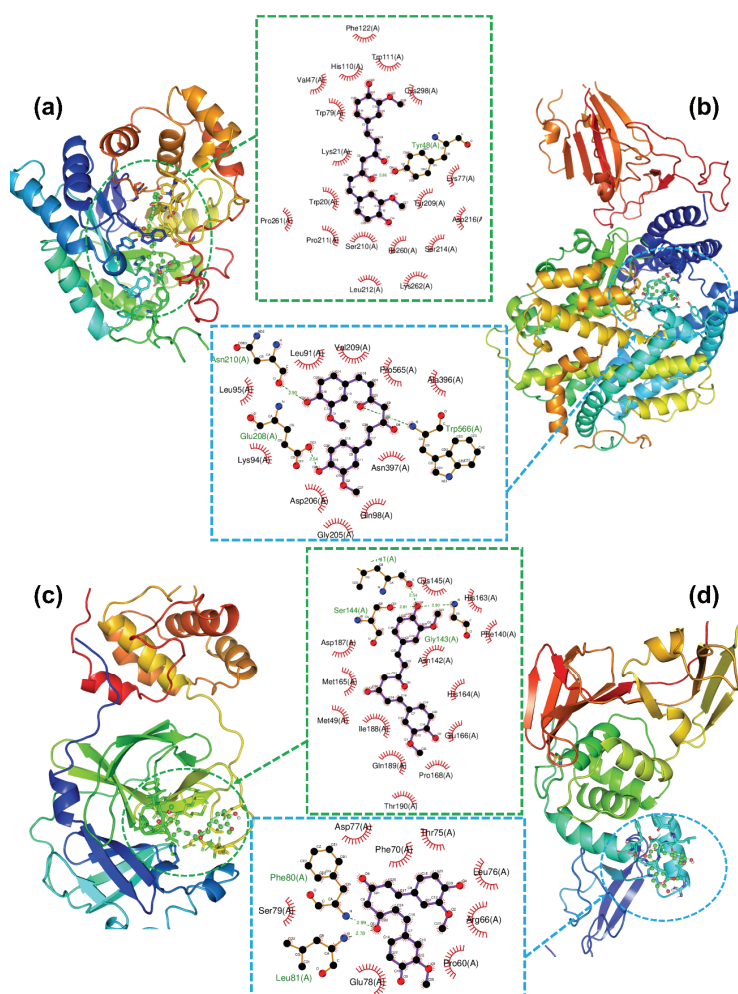

Fig. 1. Lowest binding energy docking pose of curcumin in: a) the transmembrane serine protease 2 (TMPRSS2) PDB ID: 1Z8A, b) angiotensin-converting enzyme 2 (ACE2) PDB ID: 3D0G, c) 3-chymotrypsin-like protease (3CLpro) PDB ID: 3AW0 and d) papain-like protease (PLpro) PDB ID: 3E9S.

The lowest binding energy of curcumin with TMPRSS2, ACE2, PLpro and 3CLpro are –42.34, –28.53, –33.85 and –31.33 kJ/mol, respectively. Interestingly, the most stable docking pose of curcumin has been observed with TMPRSS2. The detailed study of the four most stable docking poses of curcumin in TMPRSS2, ACE2, PLpro and 3CLpro has been reported in the supporting information. The ligand efficiency and the intermolecular energy of curcumin with TMPRSS2 are measured the highest, whereas the tortional free energy is found the same for all four complexes formed after docking. At the same time, the inhibition efficiency of curcumin with TMPRSS2 (38.37 nM) is found the lowest compared to that with ACE2 (10.0 µM), PLpro (1.18 µM) and 3CLpro (3.22 µM).

Furthermore, the docking studies show that curcumin interacts with TMPRSS2 through both hydrogen bonding (H-bonding) and dispersion interactions. Amino acids LYS21, TYR48, TRP111 and LEU212 of Chain A interacts through H--bonding and the corresponding H-bonding distance is found 4.01, 3.15, 3.72 and 3.86 Å, respectively. Interestingly, the aromatic rings of amino acid TRP21 of chain A of TMPRSS2 and curcumin interact through π–π stacking interaction with an interplanar distance of 5.49 Å, the interaction is shown in Fig. 1a. Several other amino acids interact through hydrophobic interactions. These interactions are shown in Fig. 1a. Amino acids LYS94, GLN98, TYR196, GLU208 and TRP566 of chain A of ACE2 interact with curcumin through H-bonding and the corresponding H-bonding distances are 3.92, 3.84, 3.79, 2.54 and 2.99 Å, respectively whereas other interactions have been shown in Fig. 1b. Interestingly, GLY143, SER144 and GLU189 of chain A of PLpro and ARG66, PHE80 and LEU81 of Chain A of 3CLpro interacts with curcumin through hydrogen bonding. The detailed chart of interactions in the lowest binding energy docking poses of curcumin with TMPRSS2, ACE2, PLpro and 3CLpro is shown in the supporting information. The adaptive Poisson–Boltzmann solver (ABPS), which provides the Poisson–Boltzmann electrostatic calculation, are also depicted in the Supplementary material to this paper, which shows the electrostatic interaction of curcumin with TMPRSS2, ACE2, 3CLpro and PLpro.

Amino acids GLY143, SER144 and GLN189 of chain A of PLpro interacts to curcumin through H-bonding with distance of 2.90, 2.58 and 2.56 Å, respectively. 2D and 3D representation of docking poses of curcumin with PLpro are shown in Fig. 1c. Amino acids ARG66, PHE80 and LEU81 of chain A of 3CLpro interacts to curcumin through H-bonding with distance of 3.43, 2.99 and 2.78 Å, respectively (Fig. 1d).

Structural analysis

The optimized geometry of curcumin in the gas phase (I) at B3LYP/def2--TZVP level of theory and geometries of curcumin lifted from the lowest binding energy active sites of TMPRSS2 (IIa), ACE2 (IIb), 3CLpro (IIc) and PLpro (IId)

are depicted in Fig. 2, whereas the corresponding geometrical parameters are tabulated in the Supporting material to this paper. Curcumin is an interesting molecule connected through a long chain of multiple conjugated double bonds, which provides structural flexibility to adjust in the active sites. Fig. 2 shows a surprising glimpse of this structural flexibility of curcumin in various active sites. The geometry of curcumin bends a lot in the active site of ACE2 and PLpro, in comparison to the gas phase geometry, and acquires U-shape. Interestingly, the study of geometrical parameters provides in-depth understanding about this.
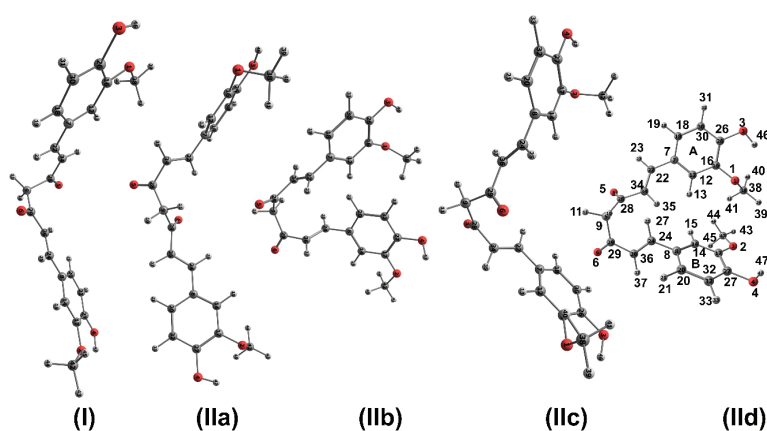

Fig. 2. Optimized geometry (I) of curcumin in gas phase at B3LYP/def2-TZVP level of theory. Geometries of curcumin lifted from the active site of TMPRSS2 (IIb), ACE2 (IIb), 3CLpro (IIc) and PLpro (IId).

The bond length of ring $C(sp^2)$–$C(sp^2)$ carbon bonds in curcumin in gas phase (I) and the same lifted from active sites (IIa, IIb, IIc, IId) are measured between 1.38–1.41 Å, whereas the bond angles inside the rings are found between 118.3––121.5°. A small change is reported in the geometrical parameters inside ring. The bond lengths of chain carbon bonds C8–C24, C36–C29, C28–C34 and C7–C22 are found to be increased by 0.02 Å in the active sites compared to that in the gas phase. The increase in bond length is attributed to intermolecular interaction with the amino acids in the active sites.

Interestingly, the major change is observed in the dihedral angles along the chain length in different forms of curcumin. Dihedral angles ∠C22–C34–C28–C9, ∠C34–C28–C9–C29, ∠C28–C9–C29–C36 and ∠C9–C29–C36–C24 in the form (I) are measured 5.2°, –80.3°, –67.5° and –177.3°, respectively. The same in the form (IIb) are –135.7°, 104.3°, –39.1° and –66.7°, respectively, whereas the same in the form (IId) are –141.1°, –93.1°, 79.3° and –5.4°, respectively. The changes in the dihedral angles are mainly responsible for the geometrical change to U--shape in IIb and IId forms, which can be observed in Fig. 2.

Atomic charge

Mulliken population analysis (MPA) charges of curcumin in the gas phase and that lifted from the active site of TMPRSS2 (IIb), ACE2 (IIb), 3CLpro (IIc) and PLpro (IId) calculated at B3LYP/def2-TZVP level of theory are reported in Fig. 3. The corresponding plot of natural population analysis (NPA) charge along with detailed data is reported in the Supplementary material. The study depicts that MPA charges of hydroxyl oxygens O3 are –0.38681e, –0.39929e, –0.39646e, –0.40884e and –0.38819e for I, IIa, IIb, IIc and IId, respectively. Similarly, MPA charges of hydroxyl oxygens O4 are –0.38775e, –0.38995e, –0.42946e, –0.39773e and –0.39995e for I, IIa, IIb, IIc and IId, respectively. It shows that MPA charge of hydroxy oxygen increases on binding with amino acids in the active site of receptor in comparison to that in the gas phase (I). Interestingly, the MPA charges of hydroxyl oxygen O3 and O4 are found lower than carbonyl oxygens, O5 and O6. At the same time the carbon atom attached to the electronegative oxygens O3, O4, O5 and O6 are C26, C27, C28 and C29, respectively, and the MPA charges of these carbons are found higher. This is prominently reported in case of NPA charges (see Fig. S7 of the Supplementary material). NPA charges for hydroxyl oxygen O3 and O4 are less than that for carbonyl oxygen O5 and O6 for all forms of curcumin, whereas an increase in NPA charges is also reported for O3, O4, O5 and O6 in case of curcumin lifted from the active sites. Overall, the comparison of atomic charges (MPA and NPA) nicely helps to understand the interaction of curcumin with TMPRSS2, ACE2, 3CLpro and PLpro.
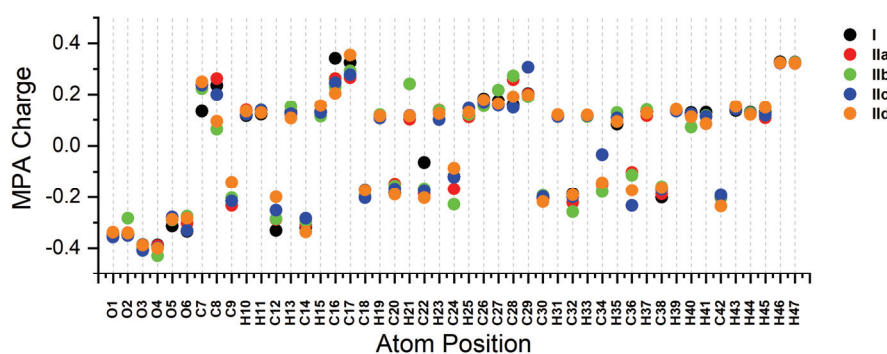

Fig. 3. Mulliken population analysis (MPA) charges of curcumin in the gas phase and that lifted from the active site of TMPRSS2 (IIb), ACE2 (IIb), 3CLpro (IIc) and PLpro (IId).

AIM analysis

Electron density ρ_{bcp} (r) and Laplacian of electron density $\nabla^2\rho_{bcp}$ (r) of curcumin in the gas phase (I) and that lifted from the active site of TMPRSS2 (IIa), ACE2 (IIb), 3CLpro (IIc) and PLpro (IId) are studied at B3LYP/def2-TZVP level

of theory and graphically represented in Fig. 4. The corresponding detailed report and figure have been added in the supporting information. An average of ρ_{bcp} (r) at the bond critical points (BCP) of carbon bonds in the two aromatic rings of curcumin (I) are 0.3191/0.3190 a.u., whereas the same of curcumin in the form IIa, IIb, IIc and IId are 0.3213/3214, 0.3207/0.3207, 0.3215/0.3210 and 0.3219//0.3202 a.u., respectively. Interestingly, the ρ_{bcp} (r) at ring critical points (RCPs) of two aromatic rings of curcumin in I form are 0.0229/0.0230 a.u., whereas the same for curcumin in IIa, IIc, IIc and IId are 0.0233/0.0232, 0.0231/0.0232, 0.0231/0.0232 and 0.0233/0.0231 a.u., respectively. It shows that the electron densities at the curcumin in the forms IIa, IIb, IIc and IId increase in comparison to that in gas phase, *i.e.*, isolated form (I) due to interaction with amino acids present in the docking site.
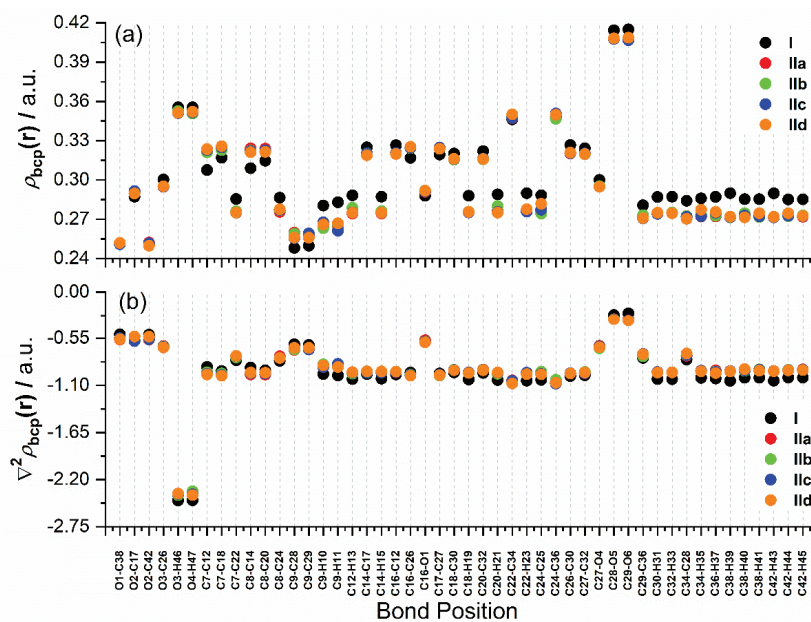

Fig. 4. Plots of: a) electron density ρ_{bcp} (r) and b) Laplacian of electron density $\nabla^2\rho_{bcp}$ (r) of curcumin in the gas phase and the same lifted from the active site of TMPRSS2 (IIa), ACE2 (IIb), 3CLpro (IIc) and PLpro (IId).

The ρ_{bcp} (r) of alcoholic bonds O3–H46 and O4–H47 are measured 0.3555//0.3555 a.u. in form (I), whereas that are in curcumin in the form IIa, IIb, IIc and IId are 0.3523/0.3520, 0.3525/0.3507, 0.3510/0.3516 and 0.3514/0.3521 a.u., respectively. A jump in ρ_{bcp} (r) of ketonic bond C28–O5 and C29–O6 are measured 0.4143/0.415 a.u. in form (I), whereas the same in curcumin lifted from the form IIa, IIb, IIc and IId are 0.4078/0.4075, 0.4078/0.4076, 0.4077/0.4068 and 0.4082//0.4087 a.u., respectively. Thus, the ρ_{bcp} (r) of alcoholic and ketonic bonds of

curcumin decreases in the active site compared to that in gas phase by 0.003 and 0.007 a.u. The H-bonding interaction is found responsible for this difference.

Sametime $\nabla^2\rho_{bcp}$ (r) for the hydroxyl groups of curcumin in the forms IIa, IIb, IIc and IId are higher than that in the gas phase (I). The difference is attributed to H-bonding interaction. The comparison of ρ_{bcp} (r) and $\nabla^2\rho_{bcp}$ (r) of the ketonic groups (C29–O6 and C28–O5) in the four different forms of curcumin defines its interaction with amino acids in the docking site.

HOMO–LUMO band gap and dipole moment measurements

The geometries of curcumin in gas phase are optimized at B3LYP/def2--TZVP level of theory while single point calculations are performed for IIa, IIb, IIc and IId at same level of theory. HOMO energy gives the impression of ionization potential relating the ability to donate an electron while LUMO energy directly correlates with electron affinity relating the ability to accept an electron. Thus HOMO–LUMO energy gap provides the information about the molecular stability. As HOMO–LUMO energy gap for a molecule decreases the polarizability and the reactivity of the molecule increases. The HOMO–LUMO calculations are performed and reported 3.699 eV in the gas phase, whereas the same obtained for IIa, IIb, IIc and IId are 4.367, 4.392, 3.714 and 4.058 eV, respectively. The band gap is found lowest at the gas phase and the band gap for IIc is measured close to gas phase but high value of band gap is measured for IIa and IIb.

Dipole moments (μ) has also calculated for all the forms of curcumin at B3LYP/def2-TZVP level of theory and reported in the supporting information. The dipole moment of curcumin in the gas phase (I) is calculated 3.26 D*, whereas dipole moments of IIa, IIb, IIc and IId are 7.022, 4.147, 4.429 and 6.8 D, respectively. The dipole moments of IIa, IIb, IIc and IId are greater than that of I, which is attributed to intermolecular interaction as well as charge distribution present close to curcumin in the active sites. Interestingly, the dipole moment of IIa is found higher than that of IIb, IIc and IId. Interestingly, the binding energy for the most preferable docking pose of curcumin with TMPRSS2 (–42.34 kJ/mol) is found lower than that in case of ACE2, PLpro and 3CLpro.

Non-covalent interaction (NCI) plot

NCI plot is helpful to understand the various non-covalent interactions present in the macromolecule. Yang and coworkers implemented reduced density gradient (RDG=$|\nabla_\rho|/2(3\pi^2)^{1/3}\rho^{4/3}$) to measure the parameters related to the non--covalent interactions in NCI plot.[35] Therefore, NCI plot is used to monitor the interaction of curcumin in the active site of TMPRSS2, ACE2, PLpro and 3CLpro. The lowest binding energy docking sites are chosen for this purpose. The closest interaction within 3.5 Å was selected using Pymol software. The

---

* 1 D = 3.34×10^{-30} C m

selected residues from TMPRSS2, ACE2, PLpro and 3CLpro along with curcu-min are used for NCI plot. Fig. 5 shows the NCI plot and underlying interactions for curcumin with the TMPRSS2, ACE2, PLpro and 3CLpro.
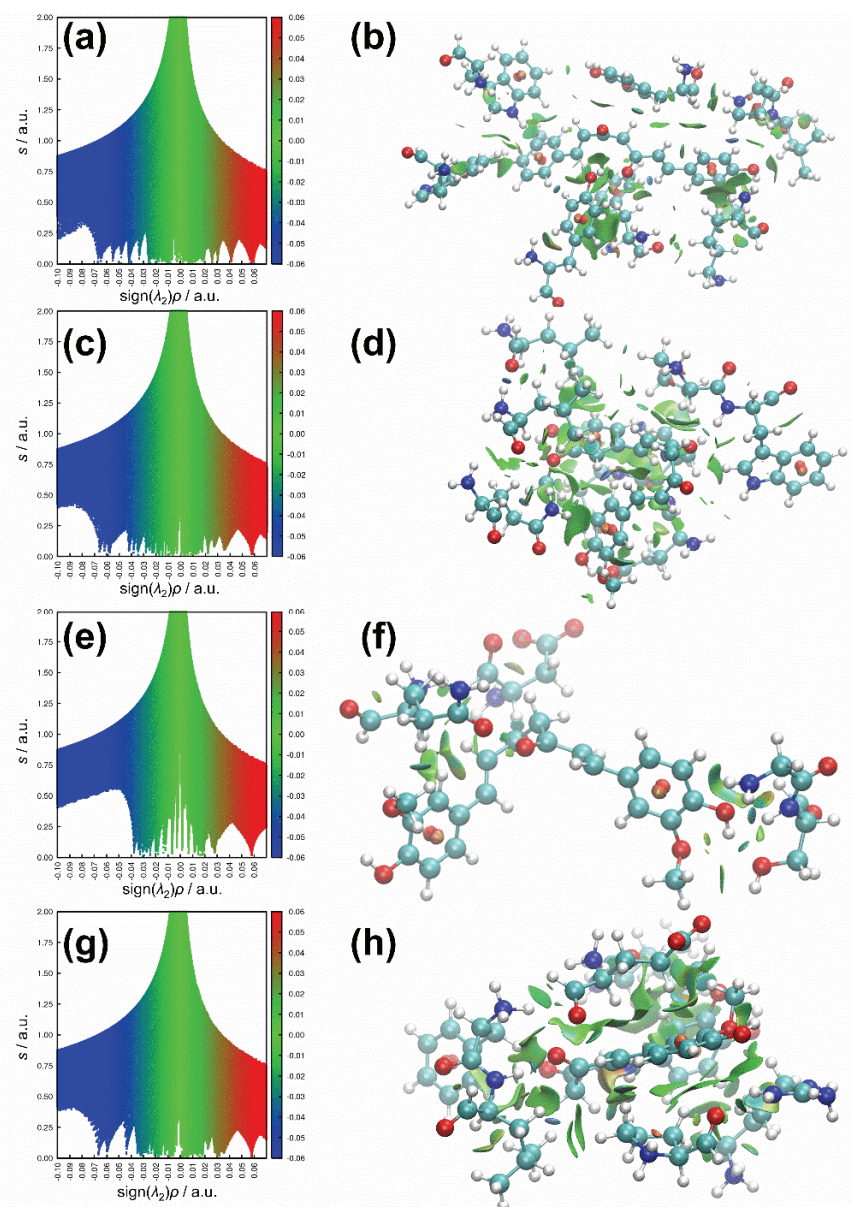

Fig. 5. RDG plot of NCI analysis for docking poses of curcumin with TMPRSS2, ACE2, 3CLpro and PLpro are plotted (a, c, e and g, respectively) along corresponding isosurface extractions of RDG plots of NCI analysis (b, d, f and h, respectively).

The coloring scheme used to discuss the isosurfaces is as follows. The blue colour indicates the strong attractive interaction. The green color indicates the interactions having intermediate strength such as H-bonding, π–π and van der Waals interactions (vdW). The red colour represents the repulsive forces. A mixture of green and blue has been mostly seen in the NCI plot, which also represents electrostatic as well as dispersion interactions. Fig. 5 (a, c, e and f) depict RDG plots of NCI analysis of docking poses of curcumin with TMPRSS2, ACE2, PLpro and 3CLpro. These plots show mostly blue and green colours indicating that the main contribution to the binding strength is originated from H--bonding and vdW interactions. The same is also confirmed through PLIP analysis.[26] The extended plots are separately shown in the supporting information for clear visibility.

Fig. 5b shows the isosurface extraction of NCI analysis showing H-bonding interaction between C=O and O–H groups of curcumin with O–H group of tyrosine and N–H group of leucine, respectively. At the same time curcumin also interacts with TRP20, TRP79, TRP111 and TYR209 through hydrogen bounding interaction in the active site of TMPRSS2P. The study support the interactions shown in Fig. 1. Fig. 5c and d shows the NCI plot and its isosurface extractions of the intermolecular interactions between curcumin and amino acids present in the active site of ACE2. Fig. 5f shows that the C=O group of curcumin interacts with N–H groups of LEU81 and PHE80 of chain A. Thus, NCI plots provided in--depth understanding of intermolecular interaction present between ligand and receptor.

CONCLUSIONS

The study of curcumin interactions with transmembrane serine protease 2 (TMPRSS2), angiotensin-converting enzyme 2 (ACE2), 3-chymotrypsin-like protease (3CLpro) and papain-like protease (PLpro) are performed using molecular docking and detailed quantum chemistry calculation. Quantum chemistry calculation provides in-depth quantitative information regarding the underlying interactions. Curcumin has multiple single bonds providing it freedom to adjust into the lowest binding energy pockets after geometrical rearrangements. The study of curcumin in the active sites has been performed through calculation of geometrical parameters, atomic charges, electron density, Laplacian of electron density, dipole moments, energy gap between highest occupied and lowest unoccupied molecular orbitals as well as NCI analysis. The study revealed that curcumin can act as a potential multiple-target inhibitor against SARS-CoV-2.

SUPPLEMENTARY MATERIAL

Additional data and information are available electronically at the pages of journal website: https://www.shd-pub.org.rs/index.php/JSCS/article/view/12081, or from the corresponding author on request.

ИЗВОД

КУРКУМИН КАО ПОТЕНЦИЈАЛНИ ИНХИБИТОР ВИШЕСТРУКИХ МЕТА ПРОТИВ SARS-COV-2 ИНФЕКЦИЈЕ: ДЕТАЉНО ПРОУЧАВАЊЕ ИНТЕРАКЦИЈЕ КОРИШЋЕЊЕМ КВАНТНО-ХЕМИЈСКИХ ИЗРАЧУНАВАЊА

SUMIT KUMAR

Department of Chemistry, Magadh University, Bodh Gaya-824234, Bihar, India

Куркумин је једно од значајних природних једињења са особинама као што су: антивирусне, антиоксидантне и противупалне. SARS-CoV-2 се појавио као заразни вирус који озбиљно угрожава велике групе становништва у свету. Било је више покушаја да се направе нова антивирусна једињења, али то је остао изазов чак и након озбиљних истраживања. Природни производ куркумин, може се користити као алтернатива антивирусним једињењима за SARS-CoV-2. Његово дејство против SARS-CoV-2 већ је истакнуто у литератури. До данас нема радова о квантитативном проучавању његове интеракције са различитим прекурсорима SARS-CoV-2. Овај чланак саопштава о интеракцији куркумина са ангиотензин-конвертујућим ензимом 2, трансмембранском серин протеазом 2, на 3-химотрипсин-налик протеазом и на папаин-налик протеазом, помоћу молекулског докинга и квантно-хемијских израчунавања, да би постигли квантитативно разумевање основа интеракција. Овде је постигнуто да и конформациона флексибилност куркумина буде расветљена, што помаже да га се смести у четири различита места за доковање. Студија је изведена коришћењем израчунавања геометријских параметара, атомсих наелектрисања, густине електрона, Лапласијана електронске густине, диполног момента и енергетског процепа између највише попуњене и најниже незаузете молекулске орбитале. Урађена је анализа не-ковалентних интеракција (NCI) да би се визуализовале слабе интеракције присутне у активним местима. Комбиновање молекулског докинга и детаљних квантно-хемијских израчунавања показује да куркумин може бити прихваћен као потенцијални инхибитор вишеструких мета против SARS-CoV-2.

(Примљено 21. септембра, ревидирано 21. новембра, прихваћено 9. децембра 2022)

REFERENCES

1. M. Cevik, M. Tate, O. Lloyd Maraolo, J. Schafers, A. Ho, *Lancet Microbe* **2** (2021) e13 (http://dx.doi.org/10.1016/S2666-5247(20)30172-5)
2. L. M. Mattio, G. Catinella, A. Pinto, S. Dallavalle, *Eur. J. Med. Chem.* **202** (2020) 112541 (http://dx.doi.org/10.1016/j.ejmech.2020.112541)
3. L. T. Lin, W. C. Hsu, C. C. Lin, *J. Tradit. Complement. Med.* **4** (2014) 24 (http://dx.doi.org/10.4103/2225-4110.124335)
4. F. A. C. Rocha, M. R. de Assis, *Phytother. Res.* **34** (2020) 2085 (http://dx.doi.org/10.1002/ptr.6745)
5. F. Zahedipour, S. A. Hosseini, T. Sathyapalan, M. Majeed, T. Jamialahmadi, K. Al-Rasadi, M. Banach, A. Sahebkar, *Phytother. Res.* **34** (2020) 2911 (http://dx.doi.org/10.1002/ptr.6738)

6. V. K. Soni, A. Mehta, Y. K. Ratre, A. K. Tiwari, A. Amit, R. P. Singh, S. C. Sonkar, N. Chaturvedi, D. Shukla, N. K. Vishvakarma, *Eur. J. Pharmacol.* **886** (2020) 173551 (http://dx.doi.org/10.1016/j.ejphar.2020.173551)

7. F. Babaei, M. Nassiri-Asl, H. Hosseinzadeh, *Food Sci. Nutr.* **8** (2020) 5215 (http://dx.doi.org/10.1002/fsn3.1858)

8. R. K. Thimmulappa, K. K. Mudnakudu-Nagaraju, C. Shivamallu, K. J. T. Subramaniam, A. Radhakrishnan, S. Bhojraj, G. Kuppusamy, *Heliyon* **7** (2021) e06350 (http://dx.doi.org/10.1016/j.heliyon.2021.e06350)

9. A. Saeedi-Boroujeni, M. R. Mahmoudian-Sani, M. Bahadoram, A. Alghasi, *Basic Clin. Pharmacol. Toxicol.* **128** (2021) 37 (http://dx.doi.org/10.1111/bcpt.13503)

10. N. Chainani-Wu, *J. Altern. Complement. Med.* **9** (2003) 161 (http://dx.doi.org/10.1089/107555303321223035)

11. Y. Huang, C. Yang, X. F. Xu, W. Xu, S. W. Liu, *Acta Pharmacol. Sin.* **41** (2020) 1141 (http://dx.doi.org/10.1038/s41401-020-0485-4)

12. H. Zhang, J. M. Penninger, Y. Li, N. Zhong, A. S. Slutsky, *Intensive Care Med.* **46** (2020) 586 (http://dx.doi.org/10.1007/s00134-020-05985-9)

13. A. Domling, L. Gao, *Chem* **6** (2020) 1283 (http://dx.doi.org/10.1016/j.chempr.2020.04.023)

14. M. Hoffmann, H. Kleine-Weber, S. Schroeder, N. Kruger, T. Herrler, S. Erichsen, T. S. Schiergens, G. Herrler, N. H. Wu, A. Nitsche, M. A. Muller, C. Drosten, S. Pohlmann, *Cell* **181** (2020) 271 (http://dx.doi.org/10.1016/j.cell.2020.02.052)

15. A. B. Jena, N. Kanungo, V. Nayak, G. B. N. Chainy, J. Dandapat, *Sci. Rep.* **11** (2021) 2043 (http://dx.doi.org/10.1038/s41598-021-81462-7)

16. A. C. Walls, Y. J. Park, M. A. Tortorici, A. Wall, A. T. McGuire, D. Veesler, *Cell* **181** (2020) 281 (http://dx.doi.org/10.1016/j.cell.2020.02.058)

17. N. Barretto, D. Jukneliene, K. Ratia, Z. Chen, A. D. Mesecar, S. C. Baker, *J. Virol.* **79** (2005) 15189 (http://dx.doi.org/10.1128/jvi.79.24.15189-15198.2005)

18. M. L. DeDiego, E. Alvarez, F. Almazán, M. T. Rejas, E. Lamirande, A. Roberts, W.-J. Shieh, S. R. Zaki, K. Subbarao, L. Enjuanes, *J. Virol.* **81** (2007) 1701 (http://dx.doi.org/10.1128/JVI.01467-06)

19. L. Kuo, P. S. Masters, *J. Virol.* **77** (2003) 4597 (http://dx.doi.org/10.1128/JVI.77.8.4597-4608.2003)

20. J. Ortego, J. E. Ceriani, C. Patino, J. Plana, L. Enjuanes, *Virology* **368** (2007) 296 (http://dx.doi.org/10.1016/j.virol.2007.05.032)

21. X. Y. Meng, H. X. Zhang, M. Mezei, M. Cui, *Curr. Comput. Aided Drug Des.* **7** (2011) 146 (http://dx.doi.org/10.2174/157340911795677602)

22. G. M. Morris, R. Huey, W. Lindstrom, M. F. Sanner, R. K. Belew, D. S. Goodsell, A. J. Olson, *J. Comput. Chem.* **30** (2009) 2785 (http://dx.doi.org/10.1002/jcc.21256)

23. M. F. Sanner, *J. Mol. Graph. Model.* **17** (1999) 57 (http://dx.doi.org/10.1016/S1093-3263(99)99999-0)

24. R. A. Laskowski, M. B. Swindells, *J. Chem. Inf. Model.* **51** (2011) 2778 (http://dx.doi.org/10.1021/ci200227u)

25. A. C. Wallace, R. A. Laskowski, J. M. Thornton, *Protein Eng.* **8** (1995) 127 (http://dx.doi.org/10.1093/protein/8.2.127)

26. M. F. Adasme, K. L. Linnemann, S. N. Bolz, F. Kaiser, S. Salentin, V. J. Haupt, M. Schroeder, *Nucleic Acids Res.* **49** (2021) W530 (http://dx.doi.org/10.1093/nar/gkab294)

27. H. M. Berman, J. Westbrook, Z. Feng, G. Gilliland, T. N. Bhat, H. Weissig, I. N. Shindyalov, P. E. Bourne, *Nucleic Acids Res.* **28** (2000) 235 (http://dx.doi.org/10.1093/nar/28.1.235)
28. M. D. Wodrich, C. Corminboeuf, P. v. R. Schleyer, *Org. Lett.* **8** (2006) 3631 (http://dx.doi.org/10.1021/ol061016i)
29. F. Weigend, R. Ahlrichs, *Phys. Chem. Chem. Phys.* **7** (2005) 3297 (http://dx.doi.org/10.1039/B508541A)
30. F. Weigend, *Phys. Chem. Chem. Phys.* **8** (2006) 1057 (http://dx.doi.org/10.1039/B515623H)
31. X. Xu, D. G. Truhlar, *J. Chem. Theory Comput.* **7** (2011) 2766 (http://dx.doi.org/10.1021/ct200234r)
32. J. Zheng, X. Xu, D. G. Truhlar, *Theor. Chem. Acc.* **128** (2011) 295 (http://dx.doi.org/10.1007/s00214-010-0846-z)
33. F. Furche, R. Ahlrichs, C. Hättig, W. Klopper, M. Sierka, F. Weigend, *Wiley Interdiscip. Rev. Comput. Mol. Sci.* **4** (2014) 91 (http://dx.doi.org/10.1002/wcms.1162)
34. C. Steffen, K. Thomas, U. Huniar, A. Hellweg, O. Rubner, A. Schroer, *J. Comput. Chem.* **31** (2010) 2967 (http://dx.doi.org/10.1002/jcc.21576)
35. E. R. Johnson, S. Keinan, P. Mori-Sanchez, J. Contreras-Garcia, A. J. Cohen, W. Yang, *J. Am. Chem. Soc.* **132** (2010) 6498 (http://dx.doi.org/10.1021/ja100936w).